

# Self-similar evolutionary solutions of self-gravitating, polytropic $\beta$ -viscous disks

S. Abbassi<sup>1</sup>, J. Ghanbari<sup>2,3</sup>, and F. Salehi<sup>2,4</sup>

<sup>1</sup> Department of Physics, Damghan University of Basic Sciences, Damghan, Iran  
e-mail: sabbassi@dubs.ac.ir

<sup>2</sup> Department of Physics, School of Sciences, Ferdowsi University of Mashhad, Mashhad, Iran

<sup>3</sup> Department of Physics and Astronomy, San Francisco State University, 1600 Holloway, San Francisco, CA 94132, USA

<sup>4</sup> Department of Physics, Khayam Institute of Higher Education, Mashhad, Iran

Received 3 January 2006 / Accepted 20 June 2006

## ABSTRACT

**Aims.** We investigate the  $\beta$ -prescription for viscosity in standard self-gravitating thin disks and predict that in a self-gravitating thin disk the  $\beta$ -model will have a different dynamical behavior compared to the well-known  $\alpha$ -prescription.

**Methods.** We used self-similar methods to solve the integrated equations that govern the dynamical behavior of the thin disk.

**Results.** We present the results of self-similar solutions of the time evolution of axisymmetric, polytropic, self-gravitating viscous disks around a new-born central object. We apply a  $\beta$ -viscosity prescription derived from rotating shear flow experiments ( $\nu = \beta r^2 \Omega$ ). Using reduced equations in a slow accretion limit, we demonstrate inside-out self-similar solutions after core formation in the center. Some physical quantities for  $\beta$ -disks are determined numerically. We compare our results with  $\alpha$ -disks under the same initial conditions. The accretion rate onto the central object for  $\beta$ -disks is greater than for  $\alpha$ -disks in the outer regions where  $\beta$ -disks are more efficient. Our results show that the Toomre instability parameter is less than one everywhere on the  $\beta$ -disk which means that in such disks gravitational instabilities can occur, so the  $\beta$ -disk model can be a good candidate for the origin of planetary systems. Our results show that the  $\beta$ -disks will decouple in the outer part of the disk where self-gravity plays an important role, in agreement with theoretical predictions.

**Key words.** accretion, accretion disks – stars: formation – planets and satellites: formation

## 1. Introduction

Accretion disks are found around many astrophysical objects, such as active galactic nuclei (AGN), binary stars and young stellar objects. Observational evidence for disks in young stellar objects gleaned both spectroscopically and through direct imaging is now quite compelling (Beckwith & Sargent 1993; Storm et al. 1993). Up to half of the solar type, pre-main sequence stars are surrounded by disks of gas and dust, many having masses similar to that expected for early solar nebula (Chandler 1998). The accretion disks around pre-main sequence stars are good candidates for the creation of planetary systems. The structure of such disks is a subject of great interest and has been studied both through self-similar solutions assuming an unsteady state (Mineshige & Umemura 1997; Mineshige et al. 1997; Tsuribe 1999) and through direct numerical hydrodynamical simulations (Igumenshchev & Abramowicz 1999; Stone et al. 1999; Torkelsson et al. 2000). It is understood that the most crucial factors are self-gravity and viscosity which play a role in angular momentum transportation on the gas disk. Accretion takes place because of dissipation which releases the free energy of the shear flow as heat, and so allows the disk material to fall deeper into the potential well of the central object. In a simple picture, Lynden-Bell & Pringle (1974) indicated that the dissipative processes must take the form of a stress that transports angular momentum outwards. It plays a significant role in many such systems, from protostellar disks to active galactic nuclei (AGN). Self-gravity will modify the radial and vertical equations and so

can influence the dynamical behavior of the accretion disks. In the standard thin accretion disk model, the effect of self-gravity is neglected, and only pressure supports the vertical structure. In contrast, the theory of self-gravitating accretion disks is less developed and in the traditional model of accretion disks, self-gravity is ignored for simplicity (e.g. Pringle 1981), although self-gravity can describe the deviation from Keplerian rotation velocity in some AGN and flat infrared spectra of some T Tauri stars. From the observational point of view, there are already some clues that the disk self-gravity can be important both in the context of proto-stellar disks and in the accretion disks around super massive black holes in the AGN. However, comparison with observations is limited by the lack of detailed models of self-gravitating disks and by an incomplete understanding of the basic physical processes involved.

The study of self-gravity in the general case is difficult and most authors usually study the effects related to self-gravity either in the vertical structure of the disk (e.g. Bardou et al. 1998) or in the radial direction (e.g. Bodo & Curir 1992). Disks in the AGN are thought to be relatively light in the sense that the ratio of  $\frac{M_d}{M_*}$  is around a few percent (where  $M$  and  $M_*$  are the masses of the disk and central star). Usually self-gravity occurs at large distances from the central objects (Shlosman & Begelman 1987), and mainly in the direction perpendicular to the plane of the disk. But in the accretion disks around young stellar objects or pre-main-sequence stars, self-gravity can be important in all parts of the disk in both vertical and radial directions. Early numerical works of self-gravitating accretion

disks began with  $N$ -body modelling (Cassen & Moosman 1981; Tomley et al. 1991). Shlosman & Begelman (1987) investigated the role of self-gravity in AGN. Recently, Ghanbari & Abbassi (2004) introduced a model that shows that self-gravity is an important effect in the equilibrium of a thick accretion disk.

Theoretical descriptions of accretion disks and these dynamics are based on the underlying physics of viscosity in the disks. Because detailed modelling of the structure and evolution of accretion disks depends on the viscosity and its dependence on the physical parameters, choosing the best viscosity model is important. There is a belief that the molecular viscosity is inadequate to describe luminous accretion disks so that some kind of turbulence viscosity is required. Most investigators adopt the so-called  $\alpha$ -model introduced by Shakura (1972) and Shakura & Sunyaev (1973) that gives the viscosity as the product of the pressure scale height in the disk ( $h$ ), the velocity of sound ( $c_s$ ) and a parameter  $\alpha$  which contains all the unknown physics. The models for the structure and evolution of accretion disks in close binary systems (e.g. dwarf novae and symbiotic stars) show that Shakura and Sunyaev's parametrization with a constant  $\alpha$  leads to results that reproduce the overall observed behavior of the disks quite well. Accretion disks treated by a weak magnetic field are subject to MHD instabilities (Balbus & Hawley 1991) that can induce turbulence in the disk, thereby transporting angular momentum and promoting accretion processes. However in many astrophysically interesting cases, such as the outer part of proto-stellar disks, the ionization level is expected to be low, significantly reducing the effect of the magnetic field in the dynamical behavior of the disk. The realization that molecular transport of angular momentum is inefficient led theoreticians to look for another mechanism of transport of angular momentum in accretion disks. A good candidate is any kind of turbulence. The  $\alpha$ -prescription is based on turbulence viscosity but there is no physical evidence for this as the origin of turbulence in the model. On the other hand, laboratory experiments of Taylor-Couette systems indicate that, although the Coriolis force delays the onset of turbulence, the flow is ultimately unstable to turbulence for Reynolds numbers larger than a few thousand (e.g., see, Richard & Zahn 1999; Hure et al. 2001). Since in all self-gravitating disks the Reynolds number is extremely high, it was thought that hydrodynamically-driven turbulent viscosity based on the critical Reynolds number probably plays a significant role in the distribution of angular momentum in the accretion disk. The resulting turbulence would then transport angular momentum efficiently. Duschl et al. (2000) have proposed a generalized accretion disk viscosity prescription based on the hydrodynamically-driven turbulence at the critical effective Reynolds number, the  $\beta$ -model, which is applied to both self-gravitating and non self-gravitating disks and is shown to yield the standard  $\alpha$ -model in the case of shock dissipation limited, non self-gravitating disks. They have shown that in the case of fully self-gravitating disks this model may explain the observed spectra of proto-planetary disks and explain the radial motion from the observed metallicity gradients in the disk galaxy.

The basic equilibrium and dynamical structure of accretion disks are now well understood, if the standard model based on the  $\alpha$ -viscosity prescription (Shakura & Sunyaev 1973) is believed. Nevertheless, it is not easy to follow its dynamical evolution, mainly because the basic equations of the system are highly non-linear, especially when the system is self-gravitating (Paczynski 1978; Fukue & Sakamoto 1992). To follow the non-linear evolution of dynamically evolving systems, in general, the technique of self-similarity is sometimes useful. Self-similar

assumptions enable us to simplify the governing equations. Self-similar solutions have a wide range of applications in astrophysics. Several classes of solutions were discussed previously (Pringle 1974; Filipov 1984), but all of them considered the disk in a fixed, central potential. But a class of self-similar solution has been provided that use self-gravity (Mineshige & Umemura 1997). These authors had found a self-similar solution for the time evolution of an isothermal, self-gravitating  $\alpha$ -viscous disk. This solution describes the homologous collapse of a disk via self-gravity and viscosity. They found that the disk structure and evolution are distinct in the inner and outer parts. The effect of self-gravity in the collapse of a polytropic self-gravitating viscous disk has been investigated by Mineshige et al. (1997).

Following the Duschl et al. (2000) suggestion for a  $\beta$ -prescription for viscosity, we apply this model for a thin self-gravitating disk around newborn stars. It may seem that using other forms of viscosity is not an important issue, because one should just change the mathematical forms of the equations. But this changes governing equations of the system that can effect the dynamical behavior of the disks. This led us to explore the self-gravitating disk using other viscosity prescriptions. However, all viscosity prescriptions have phenomenological backgrounds rather than physically confirmed backgrounds. While we do not have a clear picture of the turbulence in disks, all such prescriptions are equivalent regarding their physical backgrounds. On the other hand, self-gravitation in a disk is a highly nonlinear process as a result of the complex behaviors of the various physical agents of the system, in which the turbulent viscosity and its prescriptions play a vital role. What would happen if other forms of viscosity prescriptions in a self-gravitating disk are used? When we searched in the literature, we found the  $\beta$ -prescription as the only experimentally tested viscosity prescription. There are a few studies of the  $\beta$ -prescription compared to the  $\alpha$ -model. Many papers discuss physical considerations and applications of the  $\beta$ -model: Mayer & Duschl (2005); Weigelt et al. (2004); Pott et al. (2004); Granato et al. (2004); Mathis et al. (2004); Richard & Davis (2004). We expect to find a different dynamical behavior and we will show that gravitational fragmentation can take place everywhere in the disk. Thus it is a good description of the formation of a proto-planetary disk.

## 2. Formulation of equations for self-similar variables

Self-similar behavior provides a set of non-steady state solutions to the self-gravitating fluid equations. On the other hand, many physical problems often attain self-similar limits for a wide range of initial conditions. Also self-similar properties allow us to investigate properties of the solutions in detail, without any of the associated difficulties of numerical hydrodynamics.

### 2.1. The basic equations

In order to study the accretion processes of a thin disk under the effect of self-gravity and viscosity, we consider axisymmetric polytropic disks using cylindrical coordinates  $(r, \phi, z)$ . We assume that the accretion disks are geometrically thin in the vertical direction and symmetric in the azimuthal direction. The model is described by the fundamental governing equations:

$$\frac{\partial \rho}{\partial t} + \frac{1}{r^2} \frac{\partial}{\partial r} (r^2 \rho v_r) = 0 \quad (1)$$

$$\frac{\partial v_r}{\partial t} + v_r \frac{\partial v_r}{\partial r} - \frac{v_\phi^2}{r} = -\frac{1}{\rho} \frac{\partial p}{\partial r} - \frac{\partial \Phi}{\partial r} \quad (2)$$

$$\rho \frac{\partial (rv_\phi)}{\partial t} + \rho v_r \frac{\partial (rv_\phi)}{\partial r} = \frac{1}{r^2} \frac{\partial}{\partial r} \left( \nu \rho r^4 \frac{\partial \Omega}{\partial r} \right) \quad (3)$$

where  $\rho$ ,  $p$ ,  $v_r$  and  $v_\phi$  are density, pressure, radial and azimuthal components of velocity of the gas disk and  $\Phi$  is the gravitational potential of the gas disk inside the radius  $r$ . We assume a polytropic relation between the gas pressure and density:

$$P = K\rho^\gamma \quad (4)$$

with  $K$  and  $\gamma$  being constants. The polytropic index  $\gamma$  describes the adiabatic pressure-density relation. In subsequent analysis, we vary it and represent its effect on some physical quantities. The vertical extent of the disk at any radius is given by  $h$ , the half thickness of the disk:

$$h = \frac{c_s}{(4\pi G\rho)^{\frac{1}{2}}} = \frac{c_s^2}{2\pi G\sigma} \quad (5)$$

where  $c_s$  is the sound speed and  $\sigma$  is the surface density.

The solution of these equations, gives us the dynamical evolution of the disk which strongly depends on the viscosity model. The study of the dynamical behavior the accretion disks is postponed until more information about viscosity is available.

## 2.2. Nondimensionalization

Before we solve Eqs. (1–3), it is convenient to nondimensionalize the equations. The essence of a self-similar model is the existence of only two dimensional parameters in the problem, viz.,  $K$  and the gravitational constant  $G$ . It is assumed, and this is born out by numerical calculations, that any additional parameters, such as the initial central density, have only transient effects that quickly lost, at least in the part of the flow in which the density greatly exceeds the initial central density. If that is the case, then only one dimensionless combination of radius  $r$  and time  $t$  can be found (Mineshige et al. 1997; Yahil 1983):

$$\xi = K^{-\frac{1}{2}} G^{\frac{\gamma-1}{2}} r(t)^{\gamma-2}. \quad (6)$$

This determines the dimensionless parameterizations of any similarity solution (Mineshige et al. 1997). We consider only  $t > 0$  for our work and the origin of time ( $t = 0$ ) corresponds to the core formation epoch. Hence we have:

$$\frac{\partial}{\partial t} = \frac{\partial}{\partial t'} + (\gamma - 2) \frac{\xi}{t'} \frac{\partial}{\partial \xi} \quad (7)$$

and

$$\frac{\partial}{\partial r} = K^{-\frac{1}{2}} G^{\frac{\gamma-1}{2}} (t')^{\gamma-2} \frac{\partial}{\partial \xi} \quad (8)$$

for the transformation  $(t, r) \rightarrow (t' = t, \xi)$ . Self-similarity allows us to reduce the self-gravitating fluid equations from partial differential equations into ordinary differential equations.

To change the variables to the dimensionless form, we used  $K$  and  $G$  because we require that all of the time-dependent terms disappear in the self-similar forms of the equations. Other physical quantities (functions of  $t$  and  $r$ ) are transformed into self-similar ones (functions of only  $\xi$ ) as:

$$v_r(t, r) = K^{\frac{1}{2}} G^{\frac{1-\gamma}{2}} (t)^{1-\gamma} V_r(\xi), \quad (9)$$

$$v_\phi(t, r) = K^{\frac{1}{2}} G^{\frac{1-\gamma}{2}} (t)^{1-\gamma} V_\phi(\xi), \quad (10)$$

$$j(t, r) = KG^{1-\gamma} (t)^{3-2\gamma} J(\xi), \quad (11)$$

$$\sigma(t, r) = (2\pi)^{-1} K^{\frac{1}{2}} G^{-\frac{1-\gamma}{2}} (t)^{-\gamma} \Sigma(\xi), \quad (12)$$

$$\rho(t, r) = (4\pi\gamma)^{-\frac{1}{\gamma}} K^{\frac{1}{2}} G^{-1} (t)^{-2\gamma} \Sigma^{\frac{2}{\gamma}}(\xi), \quad (13)$$

$$p(t, r) = (4\pi\gamma)^{-1} KG^{-\gamma} (t)^{-2\gamma} \Sigma^2(\xi), \quad (14)$$

$$\nu(t, r) = KG^{1-\gamma} (t)^{3-2\gamma} \nu'(\xi), \quad (15)$$

$$m(t, r) = K^{\frac{3}{2}} G^{\frac{1-3\gamma}{2}} (t)^{4-3\gamma} M(\xi), \quad (16)$$

where

$$J = \xi V_\phi, \quad M = \frac{\xi \Sigma u}{3\gamma - 4} \quad (17)$$

with respect to another form of the continuity equation :

$$\frac{\partial m}{\partial t} + v_r \frac{\partial m}{\partial r} = 0, \quad m = 2\pi \int_0^r \sigma r dr \quad (18)$$

thus, we have

$$\dot{M} = \frac{\xi \Sigma V_r}{3\gamma - 4}. \quad (19)$$

In order to solve the equations, we need to assign the kinematic coefficient of viscosity  $\nu$ . Although there are many uncertainties about the exact form of viscosity, we employ the  $\beta$ -prescription introduced by Duschl et al.:

$$\nu' = \beta \xi V_\phi \quad (20)$$

where  $\nu'$  is in the dimensionless form. We expect that when the disk is non-self-gravitating, it leads to standard  $\alpha$ -prescriptions. Substituting this prescription into the above equations, we can investigate the dynamical evolution of the disk.

## 2.3. Transformation of the basic equations

Substituting the above transformations into Eqs. (1–3), we can introduce a set of coupled ordinary differential equations. The basic equations are then transformed into the following forms:

$$\frac{1}{\xi} \frac{d}{d\xi} (\xi \Sigma u) = (3\gamma - 4) \Sigma \quad (21)$$

$$u \frac{du}{d\xi} = -\frac{c^2}{\Sigma} \frac{d\Sigma}{d\xi} - \frac{M}{\xi^2} + \frac{J^2}{\xi^3} + (2\gamma - 3)u + (2 - \gamma)(\gamma - 1)\xi \quad (22)$$

$$u \frac{dJ}{d\xi} = \frac{1}{\Sigma \xi} \frac{d}{d\xi} \left( \beta \xi^3 \Sigma J \frac{d}{d\xi} \left( \frac{J}{\xi^2} \right) \right) + (2\gamma - 3)J \quad (23)$$

where  $u$  is defined,

$$u = V_r - (2 - \gamma)\xi \quad (24)$$

and  $c^2$  is a constant:

$$c^2 = 2(4\pi\gamma)^{\frac{1-\gamma}{\gamma}} \Sigma^{\frac{2\gamma-2}{\gamma}}. \quad (25)$$

Now we have a set of complicated differential equations that must be solved under appropriate boundary conditions. Although a full numerical solution of these equations is possible; it is more instructive to analyze the model in some restrictive cases such as slow accretion limits.

### 3. Behavior of the solutions

#### 3.1. Slow accretion limit

We consider the fluid equations for a thin disk in the slow accretion approximation. The slow accretion approximation consists of rotationally supported disks when the viscous timescale is much larger than the dynamical timescale. In addition, the pressure gradient force and the acceleration term in this approximation are ignored. The slow accretion approximation in disks has been used by Tsuribe (1999) and Minshige et al. (1997) and many others.

In the slow accretion limit ( $|V_r| \ll 1 \ll V_\phi$ ), and in Eq. (2), the Euler equation, we have a radial force-balance which means that only two terms on the right hand side of the equation balance each other:

$$\frac{J^2}{\xi^3} - \frac{M}{\xi^2} = 0. \quad (26)$$

Hence we have:

$$J = (\xi M)^{\frac{1}{2}} = \left( \frac{\Sigma u}{3\gamma - 4} \right)^{\frac{1}{2}} \xi. \quad (27)$$

We can make some simplifications in the equation of continuity in the self-similar form:

$$\frac{d \ln \Sigma}{d \ln \xi} = -1 - \frac{d \ln u}{d \ln \xi} + \left( \frac{3\gamma - 4}{u} \right) \xi. \quad (28)$$

Before deriving other equations in a slow accretion limit, we introduce the distribution of the initial specific angular momentum,  $j$ , as (Tsuribe 1999):

$$j(r) = q \frac{G}{c_s} m(r) \quad (29)$$

where  $j$  and  $m$  are the self-similar angular momentum and the total mass within the cylindrical radius  $r$ , respectively. The variable  $q$  is a dimensionless quantity that has a constant value for the invicid equilibrium solutions (Mestel 1963; Toomre 1982) and a variable value when the viscosity effect is included. Thus in dimensionless form,

$$J = qM. \quad (30)$$

Now using Eqs. (27) and (30) we find that:

$$\Sigma^{\frac{1}{2}} = \frac{(3\gamma - 4)^{\frac{1}{2}}}{qu^{\frac{1}{2}}}. \quad (31)$$

With Eqs. (23), (24), (27), (28) and (31) we find a simple differential equation for  $V_r$ :

$$\frac{dV_r}{d\xi} = \frac{q}{\beta} \frac{V_r [V_r \mp (2 - \gamma)\xi]^2}{\xi [\pm 3V_r \mp (3\gamma - 2)\xi]} + \frac{[3(2 - \gamma) \pm 5(3\gamma - 4)]V_r}{[\pm 3V_r \mp (3\gamma - 2)\xi]} + \frac{[(2 - \gamma)(-18\gamma + 22) \mp 2(3\gamma - 4)^2]\xi}{[\pm 3V_r \mp (3\gamma - 2)\xi]}. \quad (32)$$

Now we can use the standard fourth-order Runge-Kutta scheme to integrate this ordinary differential equation. We can also use the asymptotic solutions of this equation near the origin and the outer part of the disk as a boundary condition.

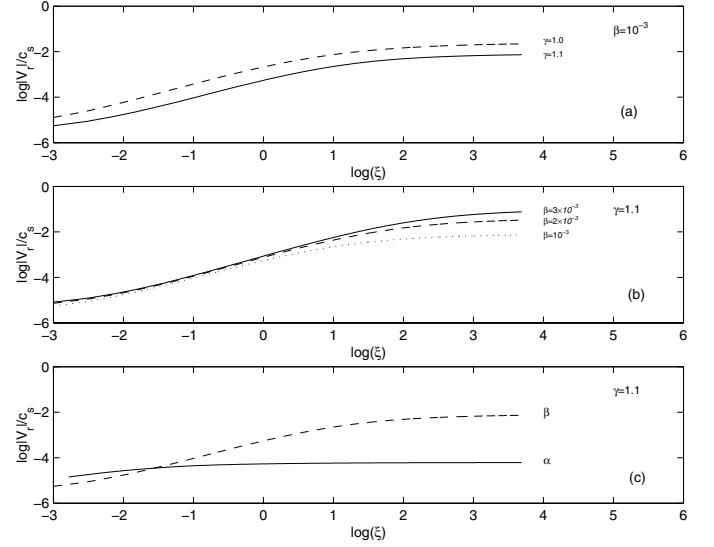


**Fig. 1.** Radial self-similar velocity distributions as a function of the self-similar variable  $\xi$  for **a)**  $\gamma = 1.0, 1.1$  at  $\beta = 10^{-3}$  **b)**  $\beta = 10^{-3}, 2 \times 10^{-3}, 3 \times 10^{-3}$  at  $\gamma = 1.1$  **c)**  $\beta = 10^{-3}$  and  $\alpha = 10^{-1}$  at  $\gamma = 1.1$ .

#### 3.2. Numerical analysis

To solve Eq. (32) numerically, we need one boundary condition. We derived asymptotic solutions in the limits  $\xi \rightarrow 0$  and  $\xi \rightarrow \infty$  for  $V_r$  where these asymptotic values can be used as the boundary condition.

$$V_r = \frac{5\gamma - 6}{6\gamma - 7} \left\{ \xi - \frac{q_0 (\gamma - 1)^2}{\beta} \xi^2 \right\} \quad \xi \rightarrow 0 \quad (33)$$

$$V_r = -\frac{\beta}{q_0} \frac{[(2 - \gamma)(22 - 18\gamma) - 2(3\gamma - 4)^2]}{(2 - \gamma)^2} \quad \xi \rightarrow \infty \quad (34)$$

where  $q_0$  is the asymptotic value of  $q$  in the outer radius. The Eq. (32) is integrated in the limits of the following equations (Eqs. (33) and (34)). It was found that only for some special values of the physical parameter such as  $q, \gamma, \beta$  does there exist physical solutions satisfied at both boundary conditions. By solving this equation we will have the  $V_r$  profile as a function of  $\xi$  and other profiles ( $V_\phi, \Sigma \dot{M}, \dots$ ) can be obtained easily. In Figs. 1 and 2, we show radial and azimuthal velocity distributions for some  $\gamma$  and  $\beta$  values. Figures 3 and 4 indicate surface densities and mass accretion rate profiles for some  $\gamma$  and  $\beta$  values. Also we compare  $\beta$  and  $\alpha$  disks for  $\gamma = 1.1$  in all figures. The self-similar variables are functions of  $\xi$ . The behavior of the solutions predicted by the beta viscosity results in higher radial velocity (see Fig. 1) than the  $\alpha$ -model (at least in the outer part of the disk where the self-gravity plays an important role) and for the azimuthal component of self-similar velocity,  $\beta$ -viscosity leads to higher velocities than the  $\alpha$ -model (see Fig. 2). Therefore, the viscosity has a greater role in the redistribution of angular momentum, and it leads to more radial flow and higher accretion rates.

It is predicted that in the outer parts of a thin, viscous disk around QSOs, self-gravity plays an important role. This effect is investigated by the Toomre parameter (Toomre 1964), such that the local gravitational instability occurs where  $Q < 1$  and where  $Q > 1$  the disk is stable against gravitational fragmentation. It is useful to calculate  $Q$  values to compare gravitational stability

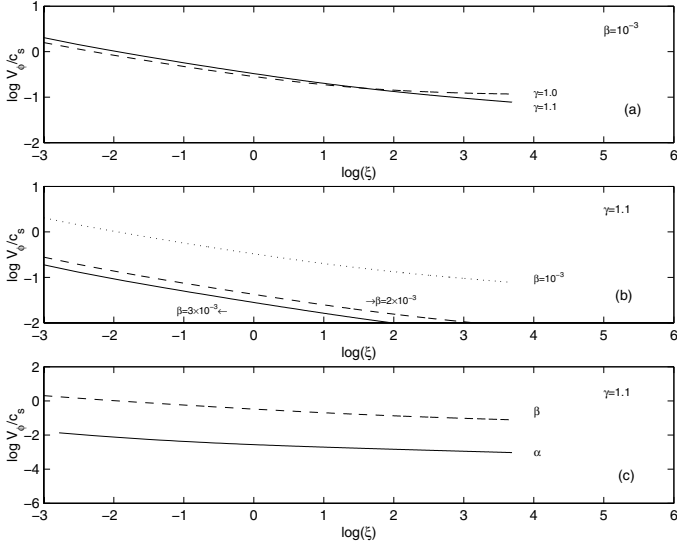


**Fig. 2.** Azimuthal self-similar velocity distributions as a function of the self-similar variable  $\xi$ , corresponding to **a)**  $\gamma = 1.0, 1.1$  at  $\beta = 10^{-3}$  **b)**  $\beta = 10^{-3}, 2 \times 10^{-3}, 3 \times 10^{-3}$  at  $\gamma = 1.1$  **c)**  $\beta = 10^{-3}$  and  $\alpha = 10^{-1}$  at  $\gamma = 1.1$ .

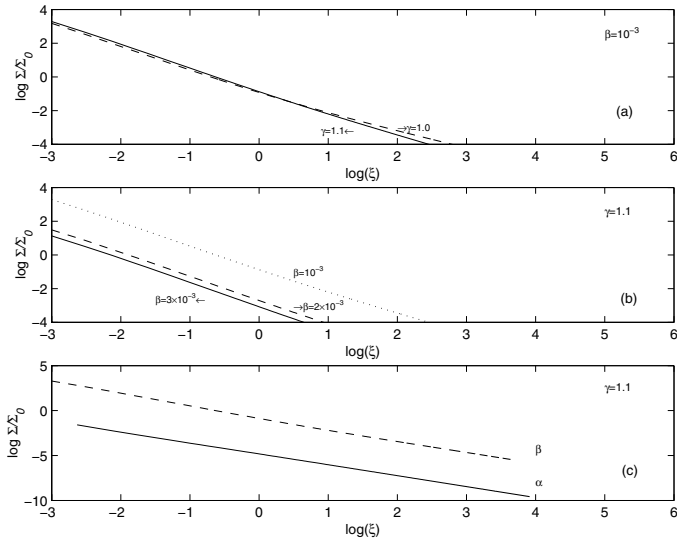


**Fig. 3.** Self-similar surface density distributions as a function the of self-similar variable  $\xi$ , corresponding to **a)**  $\gamma = 1.0, 1.1$  at  $\beta = 10^{-3}$  **b)**  $\beta = 10^{-3}, 2 \times 10^{-3}, 3 \times 10^{-3}$  at  $\gamma = 1.1$  **c)**  $\beta = 10^{-3}$  and  $\alpha = 10^{-1}$  at  $\gamma = 1.1$ .

in  $\beta$  and  $\alpha$  disks. The Toomre stability parameter for epicyclic motion is:

$$Q = \frac{c_s k}{\pi G \sigma} = \frac{2J \sqrt{2} y}{\xi^2} K^{\frac{\gamma-1}{4}} (4\pi)^{\frac{1-\gamma}{2\gamma}} \gamma^{\frac{1}{2\gamma}} \Sigma^{-\frac{1}{\gamma}} \quad (35)$$

where

$$k = \Omega \left( 4 + 2 \frac{d \log \Omega}{d \log r} \right)^{\frac{1}{2}} \quad (36)$$

is the epicyclic frequency and  $\frac{dJ}{d\xi} = \frac{J}{\xi} y$ . So if  $\gamma = 1$ , we obtain

$$Q = \frac{2J \sqrt{2} y}{\Sigma \xi^2} \quad (\text{Tsuribe 1999}).$$

In Fig. 5, we show the distribution of the Toomre  $Q$  value for some  $\gamma$  and  $\beta$  values. We also compare  $\beta$  and  $\alpha$  disks for  $\gamma = 1.1$ .

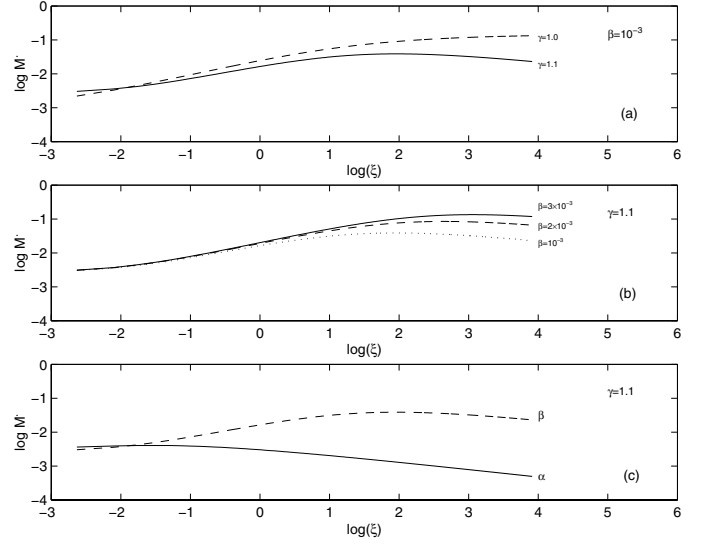


**Fig. 4.** Self-similar mass accretion rate distributions as a function of the self-similar variable  $\xi$ , corresponding to **a)**  $\gamma = 1.0, 1.1$  at  $\beta = 10^{-3}$  **b)**  $\beta = 10^{-3}, 2 \times 10^{-3}, 3 \times 10^{-3}$  at  $\gamma = 1.1$  **c)**  $\beta = 10^{-3}$  and  $\alpha = 10^{-1}$  at  $\gamma = 1.1$ .

In Fig. 6, the angular momentum coefficient  $q = \frac{J}{M}$  is plotted as a function of  $\xi$  for some  $\gamma$  values at  $\beta = 10^{-3}$ . Also we see its behavior for  $\beta$  and  $\alpha$  disks.

#### 4. Time scales

To estimate the effect of viscosity on the evolution of accretion disks we can compare the viscous time scale with the dynamical time scale. The dynamical time scale  $\tau_{\text{dyn}}$  is given by:

$$\tau_{\text{dyn}} = \frac{1}{\Omega} \quad (37)$$

where  $\Omega$  in the non self-gravitating (NSG) and Keplerian self-gravitating (KSG) framework is given by the mass of the central accretor and by the radius. But in the fully self-gravitating disks,  $\Omega$  is determined by solving Poisson's equation. The time scale of viscose evolution  $\tau_{\text{visc}}$  is given by

$$\tau_{\text{visc}} = \frac{r^2}{\nu} \quad (38)$$

where in the standard non self-gravitating and geometrically thin accretion disks where  $h \ll r$  (case  $\alpha$ -disks), this leads to

$$\tau_{\text{visc}}^{\text{non-SG}} = \left( \frac{r}{h} \right)^2 \frac{\tau_{\text{dyn}}}{\alpha} \quad (39)$$

In full self-gravitating (FSG) or KSG disks ( $\beta$ -disks) is given by

$$\tau_{\text{visc}}^{\text{FSG}} = \tau_{\text{visc}}^{\text{SG}} = \tau_{\text{visc}}^{\text{KSG}} = \frac{\tau_{\text{dyn}}}{\beta} \quad (40)$$

So with  $\alpha < 1$  and  $\beta \ll 1$ , in all circumstances  $\tau_{\text{visc}} \gg \tau_{\text{dyn}}$ . The slow accretion limit thus will be confirmed. The best approximation for the  $\alpha$  parameter in the standard accretion model is less than one,  $\alpha \sim 0.1$ , but in the  $\beta$  model which is based on the critical Reynolds number, beta is approximately  $\beta \sim 10^{-2} - 10^{-3}$ . The  $\left(\frac{h}{r}\right)$  in the outer part of accretion disks is too small, so in the outer part of the disk where self-gravity dominates the beta viscous time scale is less than the alpha viscous time scale. Therefore, the dynamical evolution of the  $\beta$ -disks at least

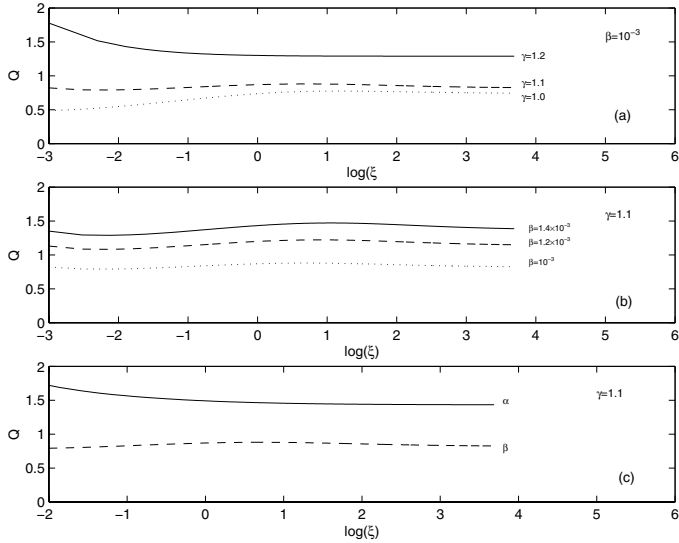


**Fig. 5.** Distribution of the Toomre  $Q$  value as a function of the self-similar variable  $\xi$ , corresponding to **a)**  $\gamma = 1.0, 1.1$  at  $\beta = 10^{-3}$  **b)**  $\beta = 10^{-3}, 2 \times 10^{-3}, 3 \times 10^{-3}$  at  $\gamma = 1.1$  **c)**  $\beta = 10^{-3}$  and  $\alpha = 10^{-1}$  at  $\gamma = 1.1$ .

in the outer part is faster than the inner parts. In the case of non-SG disks the  $\beta$ -model can recover the standard  $\alpha$ -disks. With the  $\beta$ -model we can reconstruct a more accurate picture of the equilibrium of galactic and proto-planetary disks. As we can see in Fig. 1, in comparison to the  $\alpha$  model, the radial flow in the beta disk is quite high which is relevant to the beta mechanism time scale. Because the time scale of the beta disk is shorter, it can evolve disks effectively and it can produce the large radial flow. In the case of galactic disks, the inflow velocities in the  $\beta$ -model suggests values in the range  $0.3\text{--}3 \text{ km s}^{-1}$  which is quite difficult to measure directly. The  $\alpha$ -model suggests still lower values (Duschl et al. 2000). Many authors have suggested that the radial abundance gradients observed in our own and other disk galaxies may be due to radial motion and diffusive mixing associated with the turbulence generated by eddy viscosity ( $\beta$ -disks) (Lacey & Fall 1985; Sommer-Larsen & Yoshii 1990; Koppen 1994; Edmunds & Greenhow 1995). Such radial inflows are consistent with the  $\beta$ -model, but could be described by other physical processes such as the effect of the magnetic field.

## 5. Conclusions

The  $\beta$ -prescription is based on the assumption that the effective Reynolds number of the turbulence does not fall below the critical Reynolds number. In this parametrization the viscosity is proportional to the azimuthal velocity and the radius. This yields physically consistent models of both Keplerian and fully self-gravitating accretion disks which in the case of thin disks with sufficiently small mass, recover the  $\alpha$ -disk solutions. Such  $\beta$ -disk models may be relevant for protoplanetary accretion disks (Duschl et al. 2000). In the case of protoplanetary disks they yield spectra that are considerably flatter than those due to non-self-gravitating disks, in better agreement with the observed spectra of these objects.

In this paper, we have considered the time-dependent evolution of self-gravitating disks with the  $\beta$ -prescription by a self-similar method for a thin, viscous disk. To do this, we started from dimensionless basic fluid equations. In order to consider gravity and the centrifugal force, we use the fluid equations for a

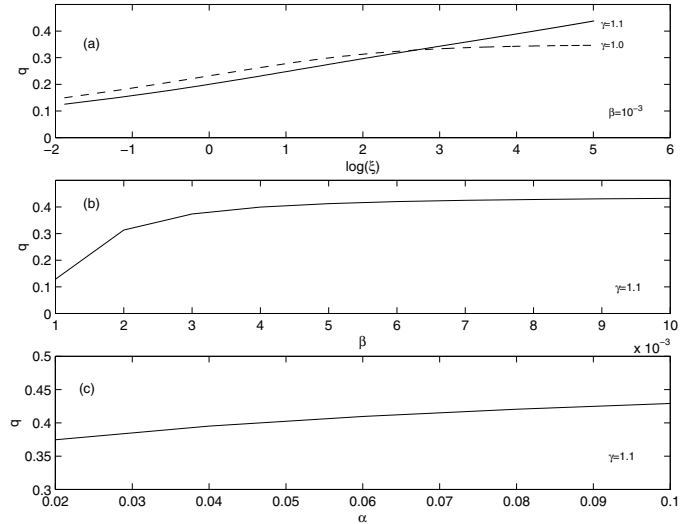


**Fig. 6.** The angular momentum coefficient profile,  $q$ , as a function the self-similar variable  $\xi$  corresponding to **a)**  $\gamma = 1.0, 1.1$  at  $\beta = 10^{-3}$ . We see its behavior versus the dimensionless viscosity parameter for **b)**  $\beta$  disks **c)**  $\alpha$  disks at  $\gamma = 1.1$ .

thin disk in the slow accretion approximation. It has been found that the evolution is described by solving a simple differential Eq. (32). We solved it numerically, beginning the asymptotic solution of this equation near the origin as a boundary condition. To obtain physical solutions from the differential equations, we have to select  $\gamma$  from a specific range of numbers.

The presented method shows that an increase of the  $\beta$  value causes the azimuthal velocity to decrease but its general distribution function does not change throughout the disk. Also, azimuthal velocities in  $\beta$ -disks are greater than in  $\alpha$ -disks (see Fig. 2). Thus we expect the  $\beta$ -disks to evolve in different ways to the  $\alpha$ -disks.

According to Fig. 4,  $\beta$ -disks have larger mass accretion rates than  $\alpha$ -disks. So, observably, we expect them to be brighter than  $\alpha$ -disks. Also, we note that with the increase of the  $\beta$  value,  $\dot{M}$  increases. Mass flow thus increases onto the central object. This implies greater radial velocity and lower surface density (see Figs. 1, 3).

Compared to  $\alpha$ -disks, the  $q$  is not a smooth distribution ( $q = \frac{J}{\dot{M}}$ ). The  $q$  values are very small in the innermost regions (see Fig. 6). They are almost constant in the outer regions. It seems in the outer part of the disk where the beta viscosity is more efficient, the angular momentum is proportional to the disk's mass inside the radius  $r$ . In order to study the effect of the self-gravity of thin  $\beta$ -disks, we plot the Toomre parameter as a function of  $\xi$ . It is obvious that the gravitational instabilities in  $\beta$ -disks are more pronounced than in  $\alpha$ -disks,  $Q < 1$ . In Fig. 5, the Toomre parameter profile can reveal this effect. It can be expected that the  $\beta$ -disk is a good model to describe planet formation around new-born stars. We showed that in the outer parts of the disk there is a difference between  $\alpha$  and  $\beta$  models. These results were predicated by Duschl et al. (2000).

In order to study model and drive a realistic picture of a thin self-gravitating disk, one must investigate the energy exchange of the disk with its environment. This requires a mechanism to transfer the thermal energy from the disk to the outside environment; thus we should add energy equations to our model. Both  $\alpha$  and  $\beta$  models are phenomenological prescriptions for disk viscosity. In an actual model of viscosity, it is possible to combine these two models and establish an exact description for

different regions of the disk. In real accretion disks, there are many important processes other than viscosity that we have neglected, for example, non-axisymmetric waves which are also expected to transport angular momentum outward. The magnetic field and its influence are neglected and sometimes magnetic braking may transport angular momentum. However, these preliminary solutions can increase our understanding of the physics governing the accretion disk.

## References

- Balbus, S., Hawly, J., 1991, *ApJ*, 376, 214  
 Bardou, A., Heyvaerts, J., & Duschl, W. J. 1998, *A&A*, 337, 966  
 Beckwith, S. V. W., & Sargent, A. I. 1993, *ApJ*, 402, 280  
 Bodo, G., & Curir, A. 1992, *A&A*, 253, 318  
 Cassen, P., & Moosman, A. 1981, *Ikarus*, 48, 353  
 Chandler, C. J. *APS Conf. Ser.*, 148, 1998  
 Duschl, W., Strittmatter, P. A., & Biermann, P. L. 2000, *A&A*, 357, 1123  
 Edmunds, M. G., & Greenhow, R. M. 1995, *MNRAS*, 272, 241  
 Filipov, L. G. 1984, *Adv. Space Res.*, 3, 305  
 Fukue, J., & Sakamoto, C. 1992, *PASJ*, 44, 553  
 Ghanbari, J., & Abbasi, S. 2004, *MNRAS*, 350, 1437  
 Granato, G. L., De Zotti, G., Silva, L., Bressan, A., & Danese, L. 2004, *ApJ*, 600, 580  
 Huré, J. M., Richard, D., & Zahn, J. P. 2001, *A&A*, 367, 1087  
 Igumenshchev, I. V., & Abramowicz, M. A. 1999, *MNRAS*, 303, 309  
 Koppen, J. 1994, *A&A*, 281, 26  
 Lacey, C. G., & Fall, S. M. 1985, *ApJ*, 290, 154  
 Lynden-Bell, D., & Pringle, J. E. 1974, *MNRAS*, 168, 603  
 Mathis, S., Palacios, A., & Zahn, J. P. 2004, *A&A*, 425, 243  
 Mayer, M., & Duschl, W. J. 2005, *MNRAS*, 358, 614  
 Mestel, L. 1963, *MNRAS*, 126, 553  
 Mineshige, S., & Umemura, M. 1997, *ApJ*, 480, 167  
 Mineshige, S., Nakayama, K., & Umemura, M. 1997, *Publ. Astron. Soc.*, 49, 439  
 Paczynski, B., *AcA*, 1978, 28, 91  
 Pott, J. U., Hartwich, M., Eckart, A., et al. 2004, *A&A*, 415, 27  
 Pringle, J. E. 1974, Ph.D. thesis, Univ. Cambridge  
 Richard, D., & Zahn, J. P., 1999, *A&A*, 347, 734  
 Richard, D., & Davis, S. S. 2004, *A&A*, 416, 825  
 Shakura, N. I. 1972, *Astron. Zhur.*, 49, 921  
 Shakura, N. I., & Sunyaev, R. A. 1973, *A&A*, 24, 337  
 Shlosman, I., & Begelman, M. C. 1987, *Nature*, 329, 29  
 Sommer-Larsen, J., & Yoshii, Y. 1990, *MNRAS*, 243, 468  
 Stone, J. M., Pringle, J. E., & Begelman, M. C. 1999, *MNRAS*, 310, 1002  
 Storm, J., Anderson, J. B. W., Carney, B. W., et al. 1993, *RMXAA*, 26, 105  
 Tomley, L., Cassen, P., Steiman-Cameron, T. 1991, *ApJ*, 382, 530  
 Toomre, A. 1964, *ApJ*, 139, 1217  
 Toomre, A. 1982, *ApJ*, 259, 535  
 Torkelsson, U., Ogilvie, G. I., Brandenburg, A., et al. 2000, *MNRAS*, 318, 47  
 Tsuribe, T. 1999, *ApJ*, 527, 102  
 Weigelt, G., Wittkowski, M., Balega, Y. Y., et al. 2004, *A&A*, 425, 77  
 Yahil, A. 1983, *ApJ*, 265, 1047